Impact of Local Strain From Selective Epitaxial Germanium With Thin Si/SiGe Buffer on High-Performance p-i-n Photodetectors With a Low Thermal Budget

W. Y. Loh, J. Wang, J. D. Ye, R. Yang, H. S. Nguyen, K. T. Chua, J. F. Song, T. H. Loh, Y. Z. Xiong, S. J. Lee, M. B. Yu, G. Q. Lo, and D. L. Kwong

***Abstract*—This letter reports on the impact of selective epitaxial germanium, specifically its local strain effects, on high-performance p-i-n photodetectors for near-infrared applications. By combining a thin compliant Si epitaxial layer (∼6 nm) with SiGe buffer (10–15 nm), we demonstrated a high-quality Ge film (∼150 nm) prepared by two-step growth. Without using high-temperature cyclic anneal, Ge films with smooth surface (root mean square = ∼0.67 nm) and low dislocation density (4×10^6 cm^{-2}) have been produced. The Si buffer locally enhances the tensile strain ($\varepsilon = 0.63\%$) in Ge while slightly suppressing the dark current by half to 0.12 μA (with circular ring area = 1230 μm^2 and spacing = 2 μm). A lateral p-i-n Ge photodetector has been demonstrated with enhanced photoresponse of ∼190 mA/W at 1520 nm and a 3-dB bandwidth of 5.2 GHz at 1 V.**

***Index Terms*—Ge-on-silicon, heterojunctions, near-infrared, optical communications, photodetector.**

I. Introduction

HETEROEPITAXY of SiGe/Ge and Ge-on-SOI is highly desired for near-infrared photodetection application due to its CMOS process compatibility and its direct bandgap at 0.8 eV and, thus, large absorption coefficient [1]. To further broaden the detection range, tensile-strained Ge photodetectors have been fabricated using either a backside silicidation-induced strain effect [2] or a two-step Ge method [3]. The two-step Ge growth induces the tensile strain (∼0.20%) in Ge [3]. When coupled with backside silicidation, Liu *et al.* have shown that the tensile strain in Ge can be increased to 0.24%, with a resulting bandgap of 0.765 eV, which is sufficient for detection up to 1620 nm [4]. Nevertheless, these types of tensile strain were globally, instead of locally, incorporated to the devices on the whole substrate. Local strain would allow us to selectively engineer the devices, for instance, only on photodetectors among all associated photonic devices on the same substrate.

Manuscript received June 18, 2007; revised August 8, 2007. The review of this letter was arranged by Editor P. Yu.

W. Y. Loh, J. D. Ye, R. Yang, H. S. Nguyen, K. T. Chua, J. F. Song, T. H. Loh, Y. Z. Xiong, M. B. Yu, G. Q. Lo, and D. L. Kwong are with the Institute of Microelectronics, Singapore 117685 (e-mail: logq@ime.a-star.edu.sg).

J. Wang and S. J. Lee are with the Institute of Microelectronics, Singapore 117685, and also with the Silicon Nano Device Laboratory, Department of Electrical and Computer Engineering, National University of Singapore, Singapore 117576.

Color versions of one or more of the figures in this letter are available online at http://ieeexplore.ieee.org.

Digital Object Identifier 10.1109/LED.2007.906814

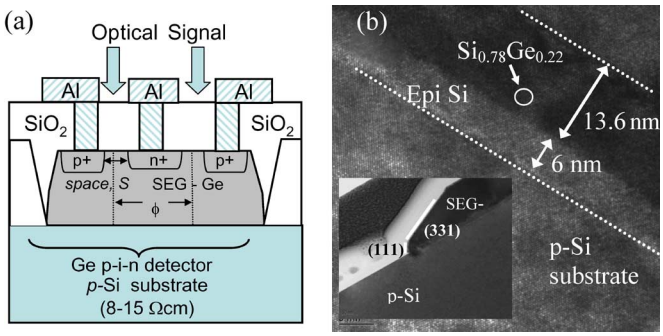

Fig. 1. Schematic diagram of normal incidence photodetectors used in this study. (a) Selective epitaxially grown Ge films on a Si substrate are patterned using a circular ring structure with lateral spacing S and diameter $\phi = 10$, 20, and 28 μm. (b) High-resolution transmission electron microscope (TEM) image of the interfacial layers for samples with a Si/SiGe buffer layer (6 nm of Si and 12 nm of SiGe). The inset shows the cross-sectional TEM view of SEG Ge on a Si/$Si_{0.8}Ge_{0.2}$ buffer layer on a p-type silicon substrate.

In this letter, the effects of selective epitaxially grown (SEG) Ge on a Si/SiGe buffer layer are investigated in terms of in-plane strain, defect density, dark current, photoresponsivity, and speed of the fabricated photodetectors. Unlike in [3] and [4], the strain effects in this study are locally incorporated based on the selective growth scheme without cyclic anneal. It is found that a Si buffer layer coupled with $Si_{0.8}Ge_{0.2}$ buffer is critical for low leakage, photoresponse, and device speed because of better film qualities and the higher tensile strain induced in the Ge layer.

II. Experimental

The schematic of the device used in this study is shown in Fig. 1(a). Ge photodetectors that are composed of dual concentric ring-shaped n^+-p^+ implants with spacing $S =$ 1.5 and 2 μm and diameter $\phi = 10$, 20, and 28 μm were fabricated. Starting with an 8-in Si p-(001) substrate (∼8–15 $\Omega \cdot$ cm), 120 nm of plasma-enhanced chemical vapor deposition (PECVD) oxide was deposited and patterned by reactive ion etching (with ∼10 nm oxide remaining) and wet dilute hydrofluoric acid (DHF, 1 : 200) etching to form an oxide window. The wafers were subsequently cleaned with standard SC1 ($NH_4OH : H_2O_2 : H_2O = 1 : 2 : 10$ at 60 °C), DHF cleaned, and isopropyl alcohol dried. All samples were then submitted for epideposition in an ultrahigh vacuum chemical vapor deposition chamber (with a base pressure $< 10^{-8}$ torr). Beginning with *in situ* N_2-bake at 800 °C after ramp-down and

stabilizing at 500 °C, a thin Si-seed layer (< 2 nm) was selectively grown with SiH_4/HCl, followed by a selective $Si_{0.8}Ge_{0.2}$ buffer layer (10–15 nm) deposition with SiH_4/GeH_4 at 400 °C. The Ge concentration of ∼21.8% was measured by energy dispersive X-ray spectroscopy (EDX), as shown in Fig. 1(b). Two different types of Ge samples with different buffer layers were prepared: Si/SiGe and SiGe buffer only. For samples with Si/SiGe buffer, an additional Si-compliant layer (6 nm) was deposited prior to the Si/SiGe buffer layer. All samples were then subjected to SEG low-temperature Ge seed (10 nm) growth at 400 °C, followed by SEG Ge (150 nm) at 600 °C, and subsequently capped with 5 nm Si with SiH_4 [5]. The Ge film surface was then patterned, implanted with As (1×10^{15} cm^{-2}/15 keV) and BF^2 (1×10^{15} cm^{-2}/15 keV), and annealed at 600 °C for 10 s to form the n^+ and p^+ junctions. Ohmic contacts were directly etched through 320 nm of PECVD oxide into the Ge n^+-p^+ region and capped with Al metallization (comprising 25 nm TaN/600 nm Al).

III. Results and Discussions

Fig. 1(b) shows the high-resolution TEM image of the SEG Ge with Si/SiGe buffer. EDX showed a very consistent Ge concentration (∼92.1%–94%) across the Ge film with Si/SiGe buffer without any trace of Si migration at various locations. For both splits, no cross-hatch pattern was observed on the Ge top surfaces. Samples with Si/SiGe buffer show a smoother surface, in which for a scanning area of 5×5 μm^2, a root-mean-square (rms) roughness value of ∼0.68 nm is obtained; whereas for those with SiGe buffer, rms roughness is ∼1.068 nm. Although the epideposition in this study was conducted in the SEG scheme, the beneficial effect of Si buffer on subsequent Ge surface conditions is consistent with that reported for blanket deposition, as in [6]. Threading dislocation (TD) is evaluated by subjecting the Ge surface to a selective etchant composed of ∼55% CrO_3 and ∼49% DHF. The estimated etch pits density (EPD) is 3.8×10^6 cm^{-2} for the sample with Si/SiGe buffer and $\sim 9.6 \times 10^6$ cm^{-2} for the one with SiGe buffer. These EPD results are comparable to the $\sim 2.3 \times 10^6$ cm^{-2} defect density obtained by Luan *et al.* using two-step Ge deposition, but with additional high-temperature cyclic anneal [7].

The film quality and in-plane strain in the Ge layers were evaluated using Raman spectroscopy with a 514.5-nm Ar^+ laser in the $z(\chi, \chi)\bar{z}$ backscattering configuration, as shown in Fig. 2. Both SiGe and Si/SiGe buffer samples show a red shift of the Ge–Ge vibrational mode compared to bulk Ge, indicating tensile strain in the SEG Ge film. The in-plane strain component can be calculated by $\Delta\omega = b\varepsilon_{\|}$, where $b = -415$ cm^{-1} using the elastic and strain tensor constant from [9]. In Fig. 2(a), it can be observed that samples with SEG Ge grown on a Si/SiGe buffer layer experience in-plane tensile strain of 0.63%. Our strain results for Si/SiGe buffer are significantly higher than that given in [4]. The major difference is the presence of low-temperature Si and SEG Ge in this study, which is expected to form a primary misfit dislocation (MD) network [10] due to the stress field during the SEG Ge growth. The underlying MD network due to the compliant microcrystalline Si layer is expected to have an even lower thermal coefficient of expansion (TCE) [11] compared to bulk Si. In contrast, samples with SiGe buffer (13.6 nm) have lower tensile strain of 0.12%. Using the parameters and theoretical formula in [12] and [13], the tensile strain in Ge after annealing at 600 °C is estimated to be 0.17%, which is close to the values obtained from samples with SiGe buffer. The enhanced tensile strain in Ge using Si/SiGe buffer results in bandgap narrowing, as shown in Fig. 2(b), which will increase photon absorption and responsivity at a longer wavelength region [3].

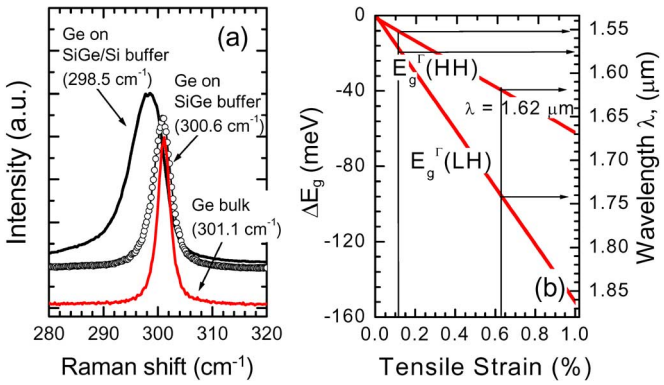

Fig. 2. (a) Micro-Raman spectroscopy of Ge films that were selectively grown on different buffer layers on a Si(001) substrate compared to a bulk Ge substrate. SEG Ge on Si/SiGe buffer shows a peak shift of 2.6 cm^{-1}, which corresponds to tensile strain of 0.63%, whereas that on SiGe buffer alone shows a lower peak shift of 0.5 cm^{-1}, which corresponds to tensile strain of 0.12%. Asymmetric broadening of the Raman spectra observed is due to the tensile strain, which causes a splitting of the threefold degeneracy of the zone center phonons into a singlet and doublet [8]. (b) Theoretical bandgap narrowing due to biaxial strain using the deformation potential calculation after [3].

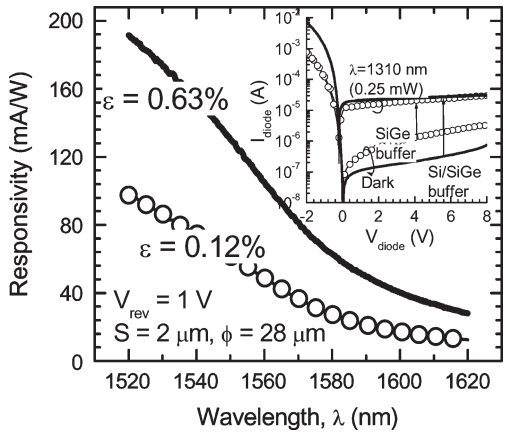

Fig. 3. Photocurrent spectral response for tensile-strained Ge p-i-n photodetectors with Si/SiGe buffer ($\varepsilon = 0.63\%$) and SiGe buffer ($\varepsilon = 0.12\%$). The inset shows the light and dark current leakage of SEG Ge on SiGe and Si/SiGe buffer layers for detectors with a diameter of 28 μm and lateral spacing of 0.2 μm. A laser with a wavelength of 1310 nm is coupled via fiber (mfd = 8 μm) onto the photodetector. Si/SiGe buffer shows a significant improvement in dark current, photoresponse, and spectral range due to enhanced tensile strain and a better Ge film quality.

Fig. 3 shows the responsivity spectra of the lateral p-i-n Ge photodetector (circular ring, with $\phi = 28$ μm and finger spacing $S = 2$ μm) under normal incidence illumination using a laser diode with a multimode fiber probe at $\lambda = 1.52$ to 1.62 μm. Samples with Si/SiGe buffer show a wider and higher photoresponse value of ∼190 mA/W at 1.52 μm compared to those with SiGe buffer, which could be attributed to the enhanced tensile strain. The responsivity is reasonable, considering the thickness of Ge (≤ 0.2 μm) and the inherent mismatch between the multimode fiber and photodiode aperture during testing. In

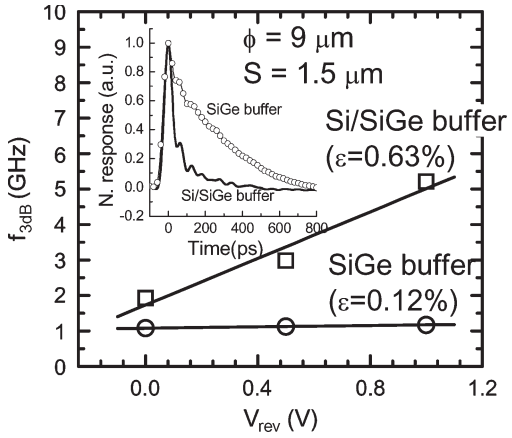

Fig. 4. FFT of the temporal response with bandwidths of 5.2 GHz (Si/SiGe buffer) and 1.17 GHz (SiGe buffer) obtained at -1 V under a normal incidence pulse from a 1550-nm fiber laser with an optical pulsewidth of 80 fs. The mobility values calculated from the FWHM transit time, i.e., $\Delta\tau_{\mathrm{FWHM}} = d/\mu\xi$, for the Si/SiGe and SiGe buffer samples are 3084 and 377 $\mathrm{cm}^2/\mathrm{V}\cdot\mathrm{s}$, respectively. The inset shows the impulse response under a 1-V reverse bias for Si/SiGe and SiGe buffer samples.

comparison, Colace *et al.* have obtained a responsivity value of 240 mA/W at 1.32 μm for a 0.4-μm-thick Ge [14]. The inset in Fig. 3 shows the leakage current of the p-i-n photodetector at 25 $^\circ$ C. Samples with Si/SiGe buffer show lower dark current and higher photocurrent $(\lambda = 1310\,\mathrm{nm})$ compared to samples with SiGe buffer due to better Ge film qualities, with lower TDs.

The temporal responses of several ring-shaped lateral detectors ($\phi = 9$ μm and electrode spacing $S = 1.5$ μm between the n^+ and p^+ regions) were measured using a 1.55-μm pulsed fiber laser (with an optical pulsewidth of 80 fs), microwave probes, and a 15-GHz sampling oscilloscope. Fig. 4 shows the pulsed response and the fast Fourier transform (FFT) for p-i-n Ge photodetectors with Si/SiGe and SiGe buffer samples. The 3-dB bandwidth is estimated to be $\sim$5.2 GHz (Si/SiGe buffer) and $\sim$1.17 GHz (SiGe buffer) at 1 V. Carrier mobility calculated from the transit time for photocurrent at a full-width at half-maximum (FWHM) pulse [14] shows that $\mu = 3084$ $\mathrm{cm}^2/\mathrm{V}\cdot\mathrm{s}$ and 377 $\mathrm{cm}^2/\mathrm{V}\cdot\mathrm{s}$ for samples with Si/SiGe and SiGe buffer, respectively. The bandwidth for the Si/SiGe buffer sample is limited by the transit time with the carrier mobility being close to the theoretical Ge mobility. As the electrode spacing is 1.5 μm wide, the highest bandwidth is limited but still comparable to the results for the Ge photodetector on a Si substrate [15]. In contrast, those of SiGe buffer shows significant speed degradation with a long transient tail. Possible reasons are carrier interactions with the higher density of traps in Ge and interface traps at the Ge/Si heterostructure for Si/SiGe buffer samples. In this case, as the secondary ion mass spectrometry analysis for SiGe and Si/SiGe shows a similar Si profile, we confirm that the degraded speed and responsivity in SiGe samples are not due to Si–Ge interdiffusion. Rather, we speculate that the higher density of traps in Ge on SiGe buffer results in an enhanced transient tail with a degraded bandwidth [16].

IV. Conclusion

We have reported on the electrical and optical characteristics of selectively grown Ge on SiGe and Si/SiGe buffer on Si for optical photodetection. Using an additional Si epitaxial layer as a buffer layer, dark current was reduced by half to 0.12 μA (with circular ring area $= 1230$ $\mu\mathrm{m}^2$ and spacing $S = 2$ μm) at 1 V with smooth surface and low dislocation density and without cyclic anneal or additional chemical–mechanical polishing. By leveraging on the MD network in the Si/SiGe buffer, the tensile strain in Ge layer is increased. A lateral p-i-n Ge photodetector that is fabricated on this Ge platform shows a photoresponsivity value of $\sim$190 mA/W at 1.52 μm and extended photon detection to a wavelength of 1.62 μm with a 3-dB bandwidth of 5.2 GHz at 1 V.

Acknowledgment

The authors would like to thank the staff in semiconductor process technologies, materials, devices, and reliability analysis, Institute of Microelectronics, Singapore, for their assistance in wafer preparation and sample analysis.

References

[1] J. M. Hartmann, A. Abbadie, A. M. Papon, P. Holliger, G. Rolland, T. Billon, J. M. Fedeli, M. Rouviere, L. Vivien, and S. Laval, "Reduced pressure-chemical vapor deposition of Ge thick layer on Si (001) for 1.3–1.55-μm photodetection," *J. Appl. Phys.*, vol. 95, no. 10, pp. 5905–5913, May 2004.

[2] J. F. Liu, D. D. Cannon, K. Wada, Y. Ishikawa, S. Jongthammanurak, D. T. Danielson, J. Michel, and L. C. Kimerling, "Silicidation-induced band gap shrinkage in Ge epitaxial films on Si," *Appl. Phys. Lett.*, vol. 84, no. 5, pp. 660–662, Feb. 2004.

[3] Y. Ishikawa, K. Wada, D. D. Cannon, J. F. Liu, H. C. Luan, and L. C. Kimerling, "Strain-induced band gap shrinkage in Ge grown on Si substrate," *Appl. Phys. Lett.*, vol. 82, no. 13, pp. 2044–2046, Mar. 2003.

[4] J. F. Liu, D. D. Cannon, K. Wada, Y. Ishikawa, S. Jongthammanurak, D. T. Danielson, J. Michel, and L. C. Kimerling, "Tensile strained Ge p-i-n photodetectors on Si platform for C and L band telecommunications," *Appl. Phys. Lett.*, vol. 87, no. 1, p. 011 110, Jul. 2005.

[5] A. Sakai, T. Tatsumi, and K. Aoyama, "Growth of strain-relaxed Ge films on Si(001) surfaces," *Appl. Phys. Lett.*, vol. 71, no. 24, pp. 3510–3512, Dec. 1997.

[6] Y. H. Luo, J. Wan, R. L. Forrest, J. L. Liu, M. S. Goorsky, and K. L. Wang, "High-quality strain-relaxed SiGe films grown with low temperature Si buffer," *J. Appl. Phys.*, vol. 89, no. 12, pp. 8279–8283, Jun. 2001.

[7] H. C. Luan, D. R. Lim, K. K. Lee, K. M. Chen, J. G. Sandland, K. Wada, and L. C. Kimerling, "High-quality Ge epilayers on Si with low threading-dislocation densities," *Appl. Phys. Lett.*, vol. 75, no. 19, pp. 2909–2911, Nov. 1999.

[8] F. Cerdeira, C. J. Buchenauer, F. H. Pollak, and M. Cardona, "Stress-induced shifts of first-order Raman frequencies of diamond-and zinc-blende-type semiconductors," *Phys. Rev. B, Condens. Matter*, vol. 5, no. 2, pp. 580–593, Jan. 1972.

[9] J. Zi, K. M. Zhang, and X. D. Xie, "Vibrational properties of Si/Ge superlattices," *Prog. Surf. Sci.*, vol. 54, no. 1, pp. 69–113, Jan. 1997.

[10] Y. B. Bolkhovityanov, A. K. Gutakovskii, V. I. Mashanov, O. P. Pchelyakov, M. A. Revenko, and L. V. Sokolov, "Plastic relaxation of solid GeSi solutions grown by molecular-beam epitaxy on the low temperature Si(100) buffer layer," *J. Appl. Phys.*, vol. 91, no. 7, pp. 4710–4714, Apr. 2002.

[11] K. Takimoto, A. Fukuta, Y. Yamamoto, N. Yoshida, T. Itoh, and S. Nonomura, "Linear thermal expansion coefficients of amorphous and microcrystalline silicon films," *J. Non-Cryst. Solids*, vol. 299–302, pp. 314–317, Apr. 2002.

[12] R. K. Tsui and M. Gershenson, "Plastic deformation and fracture resulting from stresses caused by differential thermal contraction in GaP/Si heterostructures," *Appl. Phys. Lett.*, vol. 37, no. 2, pp. 218–220, Jul. 1980.

[13] G. A. Slack and S. F. Bartram, "Thermal expansion of some diamondlike crystals," *J. Appl. Phys.*, vol. 46, no. 1, pp. 89–98, Jan. 1975.

[14] L. Colace, G. Masini, and G. Assanto, "Ge-on-Si approaches to the detection of near-infrared light," *IEEE J. Quantum Electron.*, vol. 35, no. 12, pp. 1843–1852, Dec. 1999.

[15] J. Oh, S. Csutak, and J. C. Campbell, "High-speed interdigitated Ge PIN photodetectors," *IEEE Photon. Technol. Lett.*, vol. 14, no. 3, pp. 369–371, Mar. 2002.

[16] N. R. Das and M. Jamal Deen, "Effect of interface trapping on the frequency response of a photodetector," *J. Vac. Sci. Technol. A, Vac. Surf. Films*, vol. 20, no. 3, pp. 1105–1110, May 2002.